Flow synthesis of monodisperse micron-sized polymer particles by heterogeneous polymerization using water-in-oil slug flow with non-ionic surfactant

Takaichi Watanabe[1], Kengo Karita[1], and Tsutomu Ono[1]*

(1) Department of Applied Chemistry, Graduate School of Natural Science and Technology, Okayama University, 3-1-1 Tsushima-naka, Kita-ku, Okayama, 700-8530, Japan

* Tsutomu Ono
Email: tono@okayama-u.ac.jp

Keywords: Microreactor, Heterogeneous polymerization, Slug flow, Monodisperse, Micron-sized particle

Abstract

Flow synthesis of poly(methyl methacrylate) particles were performed by heterogeneous polymerization of methyl methacrylate using a water-in-oil (W/O) slug flow with or without a non-ionic surfactant in the continuous organic phase. It was found that undesired phenomena in this polymerization system; clogging of the channel and broadening particle size distribution can be occurred when growing polymer particles adsorb to the W/O interface during polymerization, and that the addition of non-ionic surfactant to the continuous organic phase prevents the particles from adsorption to the W/O interface and gives monodisperse polymer particles. In addition, it was shown that as increasing the initiator concentration, the particle diameter becomes larger, resulting in monodisperse micron-sized polymer particles with 100% monomer conversion at 120 min reaction time. These results indicated that heterogeneous polymerization process using W/O slug flow can be a promising way to continuously prepare monodisperse polymer particles with micron-sizes in a short reaction time.

Introduction

Polymer particles with a narrow size distribution have been used in various industrial applications including inks, paintings, adhesives, liquid crystals spacers, materials for structural colors [1,2], and photonic crystals [3]. These particles have been generally prepared by heterogeneous polymerization such as emulsion polymerization [4], soap-free emulsion polymerization [5], suspension polymerization [6], and dispersion polymerization [7]. Among them, soap-free emulsion polymerization has been employed for the preparation of monodisperse submicron-sized polymer particles without any contamination of detergents on particle surface [8]. The soap-free emulsion polymerization is generally performed in the emulsion system consisting of a poorly water-soluble monomer, water-soluble initiator, and water using a batch reactor. In the polymerization, monodisperse polymer particles are formed in the water phase by the nucleation and growth mechanism through monomer diffusion from monomer droplets to the water phase [9]. The main disadvantage of soap-free emulsion polymerization is the considerably slower rate of reaction when compared to emulsion polymerization [10].

To improve the rate of polymerization, it is required to enhance the mixing and heat and mass transfer in soap-free emulsion polymerization process.

Since 1990s, tremendous effort has been devoted to the process intensification of chemical reactors using microreactors because microreactors have a large surface-to-volume ratio and short diffusion path, which provide increased heat and mass transfer efficiency [11–13] and precise controllability of temperature and reaction time [14–16]. In addition, from the viewpoint of industrial use, continuous manufacturing of products using microreactors would be worthful because the entire process is streamlined from start to finish, which enhances production efficiency and reduces manufacturing cost. Because of these advantages of the microreactors, in recent years, they have been applied to both homogeneous polymerization [17–20] and heterogeneous polymerization processes. Especially, heterogeneous polymerization using liquid-liquid multiphase systems such as emulsion polymerization [21,22], miniemulsion photopolymerization [23] and suspension polymerization [24] has been shown to be a robust way to prepare fine polymer particles with various sizes and structures.

Regarding heterogeneous polymerization using microreactors, there is a growing interest in liquid-liquid slug flow as a new type of polymerization field instead of emulsified batch, because the segmented liquid-liquid slug flow can be formed just by mixing oil and water phases in microreactors and collection of the products after polymerization can be easily done by spontaneous phase separation at the exit of the microreactors. In addition, if polymerization proceeds only in the dispersed phase of the slug flow, adhesion of polymer to channel wall could be suppressed by thin liquid film of the continuous phase formed between the dispersed phase and the inner wall of the microreactors [25]. Furthermore, it is well known that internal circulation flow generated in slug flow enhances the mixing of reactants in each slug and facilitates mass transfer between the liquid-liquid interfaces [25–29].

Recently, we have reported the production of poly(methyl methacrylate) (PMMA) particles by the soap-free emulsion polymerization of methyl methacrylate (MMA) using a water-in-oil (W/O) slug flow in a microreactor and found that the slug flow increased the rate of polymerization and gave PMMA particles with a high molecular weight (~ 1,500 kg mol^{-1}) at 20 min reaction time [30]. However, the particle size distribution of the resultant polymer particles was polydisperse (coefficient of variance, *CV* ~ 15%), which was higher than that prepared with a batch reactor (*CV* ~ 8%). In addition, although the polymerization was only occurred in the dispersed phase, the gradual onset of undesired clogging of the channel was observed over 20 min reaction time. Hence, the polymerization could not be continued over 20 min. Judging from microscopic observation of the slug flow, we presume that these issues would be caused by the adsorption of growing polymer particles in the dispersed water phase to the interface of W/O slugs. The particle adsorption to the W/O interface may lead to the formation of viscoelastic slugs similar to colloidosomes [31,32] and inhomogeneous polymerization condition within each slug, which eventually leads to polydispersity in the particle size distribution as well as clogging of the channel. If the particle adsorption to the W/O interface can be inhibited, it can be possible to produce polymer particles without channel clogging.

In this study, we develop the continuous process for the preparation of monodisperse micron-sized PMMA particles using a W/O slug flow by adding non-ionic surfactant Span 85 to the continuous oil phase. It is expected that when the slug is formed, the surfactant adsorbs to the W/O interface and then circumvents polymer particles from adsorption to the interface during polymerization. Specifically, we first investigate the change in the flow behavior of the W/O slugs near the exit of the microreactor at a reaction time just before the onset of the clogging. Then, we evaluate the effect of adding the surfactant to the continuous organic phase of the W/O slug flow on the characteristics of the polymerization as well as those of polymer particles. Finally, we examine the effect of initiator concentration on the particle size to obtain micron-sized polymer particles with a narrow size distribution. To the best of our knowledge, this is the first report to continuously prepare monodisperse polymer particles using a W/O slug flow system.

Experimental

Materials

Methyl methacrylate (MMA, FUJIFILM Wako) was used after purification by distillation under a reduced pressure to remove polymerization inhibitors. Distilled water used in all experiments was produced with a distilled water production system (RFD210TC, ADVANTEC, Japan). Sodium persulfate (NPS), dodecane, and *N, N*-dimethylformamide

(DMF), were purchased from FUJIFILM Wako and used without further purification. Span 85, which is an oil-soluble non-ionic surfactant, was purchased from Sigma-Aldrich and used without further purification.

Fabrication of a microreactor system

The microfluidic device was fabricated by assembling a T-shaped poly(1,1,2,2-tetrafluoroethylene) (PTFE) union (outer diameter 1/16”, GL science) and PTFE tube (inner diameter: 1 mm and outer diameter: 1/16”, GL science). The inlet PTFE tube having 20 cm-long was connected to syringes (HSW NORM-JECT® Syringe, Henke-Sass, Wolf) placed on syringe pumps (Harvard Pump 33 Dual Syringe Pump, Harvard Apparatus). The outlet PTFE tube was coiled helically and dipped in an oil bath (PAIRSTIRRER PS-1000, EYELA) at 70 °C. The exit of the outlet tube was placed in the collection vial put in an ice bath.

Heterogeneous polymerization of MMA using a W/O slug flow

Fig. 1 shows the experimental setup for heterogeneous polymerization of MMA using a W/O slug flow in the microreactor. For the initiator solution (W), an aqueous solution dissolving 1.0, 5.0, or 10 mmol L^{-1} (mM) of sodium persulfate (NPS) was prepared in a vial. For the organic solution (O), a mixture of MMA and dodecane [MMA/dodecane = 1/4 (v/v)] with or without non-ionic surfactant, Span 85, at the concentration of 1, 5, or 10 wt% was prepared in each vial. It is noted here that the reason why we added dodecane to the organic phase was that the dodecane in the organic phase was employed as an inert oil to keep the slug flow during polymerization. Then, these solutions were separately loaded into the disposable plastic syringes. Both syringes were placed onto the syringe pump (Harvard Pump 33 Dual Syringe Pump, Harvard Apparatus) and the tip of the syringes were connected to the inlet tubes of the microreactor. The solutions were then infused into the microreactor with a total flow rate at 184.6 μL min^{-1}, while keeping the volume ratio of organic to water phase constant at 1.0. When meeting the organic and water phases at the T-shaped union having hydrophobic surface, W/O type slug flow at the pitch distance of 1.0 mm was spontaneously formed. Then, the W/O slug flow traveled downstream and passed through the reaction region where the tube was placed in an oil bath (PAIRSTIRRER PS-1000, EYELA) at 70 °C. Each slug was quickly heated to 70 °C because of the narrow width of the microreactor. Subsequently, polymerization reaction was initiated in the dispersed water phase and proceeded during which the slugs passed through the reaction zone. To adjust the reaction time from 5 to 120 min, the length of the tube immersing into the oil bath was changed from 1.2 to 28 m, while keeping the total flow rate constant. (Table S1). After the polymerization, the sample solution was collected in a sample vial (10 mL, LABORAN) placed in an ice bath. The collected sample was subsequently phase-separated between aqueous phase and organic phase in the sample vial and the reaction was quenched. After the upper organic phase was removed from the sample, polymer particles dispersed in the lower aqueous phase were washed with pure water 3 times and collected by centrifugation (himac CF 15R, HITACHI, 15,000 rpm for 10 min). The collected polymer particles were freeze-dried overnight. All polymerization results were summarized in Table S2 to Table S7 in the supporting information.

Preparation of W/O Pickering emulsion using PMMA particles

A W/O type Pickering emulsion was prepared using PMMA particles having an average diameter of 311 nm (*CV* = 11.2%) as a stabilizer. To prepare the Pickering emulsion, a mixture consisting of 2.5 mL of deionized water, 2.5 mL of dodecane, and 0.295 g of the particles was prepared in a 10 mL vial and then the mixture was stirred by hand for a few seconds to prepare a W/O emulsion. The emulsion was then observed with an optical microscope (BX51, Olympus, Japan) at different time points (1, 3, and 72 h).

Characterization

The morphology of prepared particles after drying was observed by means of a scanning electron microscope (SEM, S-4700, Hitachi Ltd., Japan) at a voltage intensity of 2 kV. Before SEM observation, the prepared particles were sputter-coated (E-1030 Ion-Sputter, Hitachi Ltd., Japan) with Pd/Pt for 1 min to reduce the sample charging. Average particle diameter and the size distribution were determined with SEM images by using an image analysis software (WinROOF, Mitani Co., Ltd., Japan). In the image analysis, the size distribution was evaluated as the coefficient of variation (*CV*) that is defined as the ratio of standard deviation to average diameter. The *CV* values were calculated from the average diameter of 200 particles. The upper organic phase after phase separation in the collection vial were dissolved in hexane prior to measuring the monomer conversion. The monomer conversion was then measured by means of a gas chromatography (GC-14A, Shimadzu Ltd., Japan) equipped with a J&W Scientific 30 m DB-WAX column with a Shimadzu CR51 Chromatopac. The GC conditions were as follows: initial column oven temperature 40 °C, initial hold time of the column oven temperature 2 min, heating rate 10 °C min^{-1}, final column oven temperature 160 °C, final hold time 2 min, detector temperature 250 °C, and injector temperature 250 °C. The weight-average molecular weight (M_w), number-average molecular weight (M_n), and molecular-weight dispersity (M_w/M_n) were characterized using a gel permeation chromatography (HLC-8120 GPC, Tosoh Ltd., Japan), equipped with a refractive index detector and columns (TSK guard column Super H-H, TSKgel Super HM-H, and TSKgel Super H2000, TOSOH, Japan). DMF was used as the eluent at a flow rate of 0.6 mL min^{-1}. The polystyrene standard was used to make a calibration line. The interfacial tensions between organic and water phases were measured by the Wilhelmy plate method at 20 °C. As an organic phase, mixtures of 20 vol% MMA, 80 vol% dodecane, and different concentrations of Span 85

(1, 5, and 10 wt%) were used, while an aqueous solution dissolving 5 mM NPS was used as a water phase. The zeta potential of polymer particles was determined by Laser Doppler Microelectrophoresis technique using Zetasizer Nano ZS (Malvern instruments, UK) at 25 °C. The particles were suspended in water and sonicated thoroughly prior to the measurement to prepare a homogeneous suspension. The experimental values were calculated as the average of three different particle formulations.

Results and Discussion

(Figure 2)

To confirm the difference in flow behavior of W/O slug flow before and after onset of the channel clogging, we first performed the heterogeneous polymerization of MMA using a W/O slug flow in the absence of surfactant for different reaction times. After formation of the W/O slug flow at the T-shaped junction, polymerization was initiated when the slug flow entered the heating zone (Fig. 1). As shown in the inset image of Fig. 1, it was confirmed that the color of the dispersed water phase in the W/O slug flow during polymerization changed from transparent to white regardless of the reaction time, which indicates that the polymerization proceeded only in the dispersed water phase.

Fig. 2a shows the representative photographs of the exit tube of the microreactor at different reaction times (less than or longer than 20 min). When reaction time was less than 20 min, the W/O slug flow was highly stable until it reached the exit of the tube (Fig. 2a, left). The slugs released from the exit tube were subsequently phase separated to transparent organic phase and whitish water phase containing a large amount of polymer particles. In contrast, when the reaction time was longer than 20 min, slug mobility became unstable during travelling downstream, and stagnation of the slugs was observed near the exit of the tube (Fig. 2a, right). In addition, after the slugs were released from the exit tube, each dispersed water phase containing a large amount of polymer particles was not spontaneously redispersed even in the lower water phase of the collected sample, and their appearance was slug-shaped viscoelastic droplets similar to colloidosomes (Fig. 2b). Furthermore, different from the conventional soap-free emulsion polymerization of MMA using a batch reactor, the resultant polymer particles obtained using the W/O slug flow were polydisperse ($CV \sim 11–16\%$) regardless of the reaction time (Fig. 2c), even though there are many reports that polymerization using microreactor provides uniform reaction condition and thus well-defined polymers [17–24, 33,34]. Based upon these results, we speculated that the broader particle size distribution would be due to the formation of inhomogeneous reaction condition arising from the adsorption of growing polymer particles in the dispersed water phase to the W/O slug interface. We also speculated that polymer particle adsorption to the W/O slug interface could trigger the formation of slug-shaped colloidosomes, which may lead to polymer particles with a broader size distribution as well as channel clogging.

Then, we considered that if the growing polymer particles adsorb to the W/O interface of the slug flow, they should acquire surface activity during polymerization and the resultant polymer particles should also possess surface activity. To investigate whether the obtained PMMA particles show surface activity, we performed the preparation of a W/O Pickering emulsion using the PMMA particles prepared with the slug flow as a colloidal stabilizer. Fig. S1 shows the optical microscopy images of the prepared Pickering emulsion using PMMA particles having an average diameter of 311 nm (CV = 11.2%) as a stabilizer at different time points after the preparation. We confirmed the formation of the Pickering emulsion and that the resultant Pickering emulsion was highly stable at least for 72 h. These results suggest that the growing PMMA particles in the W/O slug acquire surface activity during polymerization and they could adsorb to the W/O slug interface, leading to the formation of slug-shaped colloidosomes. We also assumed that the surface activity of the PMMA particles would be originated from the surface charge of ionic end groups of the initiator molecules. Considering the above results, we next hypothesized that if the adsorption of growing PMMA particles to the W/O slug interface during polymerization will be prevented, the formation of inhomogeneous reaction condition and eventual channel clogging will be avoidable, which will make it possible to continuously produce monodisperse PMMA particles having a high monomer conversion.

To prevent growing PMMA particles from adsorption to the W/O slug interface during polymerization, we attempted to decrease the interfacial tension of the W/O interface by adding surfactant to the continuous organic phase of the W/O slug flow. As a model surfactant, we chose Span 85 because it is oil-soluble and non-ionic surfactant, and these physicochemical properties would be helpful to circumvent the following two possible phenomena; the concurrent emulsion polymerization of MMA in micelles formed by self-assembled water-soluble surfactants in the dispersed water phase and the formation of ion complex with negative charged PMMA particles *via* electrostatic forces.

(Figure 3)

(Table 1)

To investigate the effects of addition of Span 85 to the continuous organic phase of the W/O slug flow on the particle diameter, particle size distribution (*CV*), and monomer conversion, we performed the heterogeneous polymerization of MMA using the W/O slug flow with different concentrations of Span 85 (1, 5, and 10 wt%) in the continuous organic phase. The particle diameter tended to become bigger as increasing the reaction time (Fig. 3a). More importantly, different from the polymerization system in the absence of surfactant, the polymerization could proceed without channel clogging at least for 45 min, regardless of the Span 85 concentration. This is because the W/O interface of the slug flow is stabilized by Span 85 molecules, which makes it difficult for growing PMMA particles to adsorb to the interface during polymerization. It was also found that when using Span 85 at the concentration of 5 or 10 wt%, the *CV* values were considerably smaller than those at 1 wt% (Fig. 3b). This result suggests that uniformity in particle diameter is also enhanced by increasing Span 85 concentration. We consider that as increasing Span 85 concentration in the system, the number of Span 85 molecules covering with the W/O interface increases and growing PMMA particles are more difficult to adsorb to the W/O slug interface, which results in the formation of uniform reaction condition within each slug for the particle growth reaction. We also confirmed that as increasing Span 85 concentration in the W/O slug, the interfacial tension decreased, while there was no significant change in the zeta-potential of the PMMA particles (**Table 1**). These results indicate that Span 85 contributes to stabilization of W/O slug interface but is not involve in the resultant PMMA particles. Hence, we regard this polymerization as an analogue of soap-free emulsion polymerization even though the system contains Span 85 as a surfactant.

Fig. 3c shows the effect of Span 85 concentration on the monomer conversion as a function of reaction time. Among three different Span 85 concentrations, the monomer conversion was the highest and reached 81.5% at 45 min when the Span 85 concentration was 5 wt%. On the other hand, the monomer conversion was the lowest and reached only 31.3% at 45 min when the Span 85 concentration was 10 wt%. The low monomer conversion would be caused by unstable slug formation and coalescence of slugs. The decrease in the interfacial tension as increasing Span 85 concentration would cause both instability of slug flow and coalescence of slugs. These phenomena could lead to insufficient internal circulation flow in the slugs, resulting in low monomer conversion.

Fig. 3d shows SEM images of the PMMA particles prepared with different Span 85 concentrations at different reaction times. In all conditions, the morphologies of the PMMA particles were non-spherical structures with a rough surface. Although we have not elucidated the reasons, these characters can be derived from heterocoagulation during particle growth stage: the particle growth occurs through the rapid deposition of tiny particles generated freshly in the bulk on the surface of larger particles [35,36] and inhomogeneous deposition of the tiny particles may lead to polymer particles possessing non-spherical structures with a rough surface. Such particle structures can be also observed when using a batch reactor as we previously reported [30]

Based on these results, we concluded that the addition of Span 85 to the continuous organic phase of the W/O slug flow for the heterogeneous polymerization of MMA decreased the interfacial tension and effectively prevented growing polymer particles from adsorption to the W/O interface, which lead to monodisperse PMMA particles without clogging of the channel. We also found that the suitable concentration of Span 85 to prepare monodisperse PMMA particles with the highest monomer conversion was 5 wt%. Hence, we decided to fix the Span 85 concentration at 5 wt% in the following experiment.

(Figure 4)

Controlling the diameter of polymer particles while keeping a narrow particle size distribution is significantly important to apply the technology to the broad spectrum of applications. Especially, simple bottom-up polymerization systems including emulsion polymerization and dispersion polymerization would be difficult to prepare larger particles over 500 nm in diameter. Considering the mechanism of soap-free emulsion polymerization, in this system, it can be expected that particle size can become larger by increasing the ionic strength of the reaction system. Since the ionic strength is derived from the concentration of ionic initiator dissolving in water phase, we investigated the effect of initiator concentration in the dispersed water phase on the heterogeneous polymerization of MMA using a W/O slug flow with 5 wt% Span 85 in the continuous organic phase. Fig. 4a shows the effect of the initiator concentration on the particle diameter as a function of time. We confirmed that regardless of the initiator concentration, polymerization could be performed for at least 120 min without clogging of the channel. As we expected, the particle diameter increased with increasing the initiator concentration when compared at each reaction time. As increasing the charged initiator concentration, the large number of oligomers formed in higher ionic strength environment would lead to the formation of more unstable precursor particles and the precursor particles would contribute to the growth of larger particles by heterocoagulation. That is why particles became larger as increasing the initiator concentrations. In addition, it should be worth noting that in case of the initiator concentration at 10 mM, the diameter of the PMMA particles reached about 1 μm at 120 min. This result indicates a higher particle growth rate compared to the conventional batch process [37]. Fig. 4b shows the changes in the

CV value of the PMMA particles prepared with different initiator concentrations as a function of reaction time. Regardless of the initiator concentration, the *CV* values decreased as increasing the reaction time from 0 to 20 min, after which they increased again and finally reached plateau values with less than 10%, which is indication of a narrow size distribution. This tendency is well-known as self-sharpening effect [38]. The early particle coagulation can reduce the initial particle number and result in enlarging average particle size. On the other hand, the early particle coagulation also increases the completive growth process of different particles, which narrows the particle size distribution of the final particles [39]. As shown in Fig. 4c, the rate of polymerization was higher as increasing the initiator concentrations and the monomer conversion reached almost 100% in each initiator concentration at 120 min. The reason why the rate of polymerization was enhanced by increasing the initiator concentration is that as increasing the initiator concentration, the larger number of oligomers are formed in the early stage of the polymerization and they consume monomers by growth reaction.

Based on these results, we concluded that the particle diameter can be tuned from submicron-scale to micron-scale while keeping a narrow particle size distribution by changing the initiator concentration in the heterogeneous polymerization of MMA using a W/O slug flow in the presence of Span 85 (Fig. 4d). We also found that monodisperse micron-sized PMMA particles with 100% monomer conversion are obtained at 120 min using this system. Although further study will be required to demonstrate the versatility and scalability of heterogeneous polymerization process using W/O slug flow, we believe that this polymerization system can be a promising way for the continuous production of monodisperse polymer particles with micron sizes in a short reaction time.

Conclusion

We have developed a continuous flow process for the production of monodisperse micron-sized PMMA particles by a heterogeneous polymerization of MMA using a W/O slug flow in a microreactor. We found that the addition of Span 85 to the continuous organic phase of the slug flow prevents growing particles from the adsorption to the W/O interface and channel clogging, which gives uniform reaction condition in each slug during polymerization and results in monodisperse PMMA particles. We also found that the suitable Span 85 concentration should be 5 wt% to produce monodisperse PMMA particles with higher monomer conversion, and that increasing the initiator concentration provides larger particles. Using the slug flow process with the aid of Span 85, we succeeded in the continuous production of monodisperse micron-sized PMMA particles with 100% monomer conversion at 120 min reaction time.

Funding

The authors received no financial support for the research.

Conflicts of interest

The authors declare that they have no conflict of interest.

Availability of data and material

All data generated or analyzed during this study are included in this article and its electronic supplementary material.

References

[1] Kawamura A, Kohri M, Morimoto G, Nannichi Y, Taniguchi T, Kishikawa K (2016) Full-color biomimetic photonic materials with iridescent and non-iridescent structural colors. Sci Rep 6: 33984. DOI: 10.1038/srep33984.

[2] Kohri M, Yanagimoto K, Kawamura A, Hamada K, Imai Y, Watanabe T, Ono T, Taniguchi T, Kishikawa K (2018) Polydopamine-based 3D colloidal photonic materials: structural color balls and fibers from melanin-like particles with polydopamine shell layers. ACS Appl Mater Interfaces 10: 7640-7648. DOI: 10.1021/acsami.7b03453.

[3] Mikosch A, Ciftci S, Kuehne AJC (2016) Colloidal crystal lasers from monodisperse conjugated polymer particles via bottom-up coassembly in a sol–gel matrix. ACS Nano 10: 10195-10201. DOI: 10.1021/acsnano.6b05538.

[4] Schoth A, Adurahim ES, Bahattab MA, Landfester K, Muñoz-Espí R (2016) Waterborne polymer/silica hybrid nanoparticles and their structure in coatings. Macromol React Eng 10: 47-54. DOI: 10.1002/mren.201500029.

[5] Shibuya K, Nagao D, Ishii H, Konnno M (2014) Advanced soap-free emulsion

polymerization for highly pure, micron-sized, monodisperse polymer particles. Polymer 55: 535-539. DOI: 10.1016/j.polymer.2013.12.039.

[6] Yuan HG, Kalfas G, Ray WH (1991) Suspension polymerization. J Macromol Sci C 31: 215-299. DOI: 10.1080/15321799108021924.

[7] Kawaguchi S, Ito K (2005) Dispersion polymerization. Adv Polym Sci 175: 299-328. DOI: 10.1007/b100118.

[8] Nagao D, Sakamoto T, Konno H, Gu S, Konno M (2006) Preparation of micrometer-sized polymer particles with control of initiator dissociation during soap-free emulsion polymerization. Langmuir 22: 10958-10962. DOI: 10.1021/la061451l.

[9] Song Z, Poehlein GW (1989) Particle nucleation in emulsifier-free aqueous-phase polymerization: Stage 1. J Colloid Interface Sci 128: 486-500. DOI: 10.1016/0021-9797(89)90364-0.

[10] Dobie CG, Boodhoo KVK (2010) Surfactant-free emulsion polymerisation of methyl methacrylate and methyl acrylate using intensified processing methods. Chem Eng Process 49: 901-911. DOI: 10.1016/j.cep.2010.08.005.

[11] Wang K, Lu YC, Xia Y, Shao HW, Luo GS (2011) Kinetics research on fast

exothermic reaction between cyclohexanecarboxylic acid and oleum in microreactor. Chem Eng J 169: 290-298. DOI: 10.1016/j.cej.2011.02.072.

[12] Jensen KF (2001) Microreaction engineering – is small better? Chem Eng Sci 56: 293-303. DOI: 10.1016/S0009-2509(00)00230-X.

[13] Kashid MN, Renken A, Kiwi-Minsker L (2011) Influence of flow regime on mass transfer in different types of microchannels. Ind Eng Chem Res 50: 6906-6914. DOI: 10.1021/ie102200j.

[14] Hessel V, Lowe H (2005) Organic synthesis with microstructured reactors. Chem Eng Technol 28: 267-284. DOI: 10.1002/ceat.200407167.

[15] Belimov M, Metzger D, Pfeifer P (2017) On the temperature control in a microstructured packed bed reactor for methanation of CO/CO_2 mixtures. AIChE J 63: 120-129. DOI: 10.1002/aic.15461.

[16] Casquillas GV, Fu C, Le Berre M, Cramer J, Meance S, Plecis A, Baigl D, Greffet JJ, Chen Y, Piel M, Tran PT (2011) Fast microfluidic temperature control for high resolution live cell imaging. Lab Chip 11: 484-489. DOI: 10.1039/c0lc00222d.

[17] Nagaki A, Nakahara Y, Furusawa M, Sawaki T, Yamamoto T, Toukairin H,

Tadokoro S, Shimazaki T, Ito T, Otake M, Arai H, Toda N, Ohtsuka K, Takahashi Y, Moriwaki Y, Tsuchihashi Y, Hirose K, Yoshida J (2016) Feasibility study on continuous flow controlled/living anionic polymerization processes. Org Process Res Dev 20: 1377-1382. DOI: 10.1021/acs.oprd.6b00158.

[18] Junkers T (2017) Precise macromolecular engineering via continuous-flow Synthesis techniques. Macromol Chem Phys 218: 106-110. DOI: 10.1556/1846.2017.00030.

[19] Song Y, Shang M, Li G, Luo ZH, Su Y (2018) Influence of mixing performance on polymerization of acrylamide in capillary microreactors. AIChE J 64: 1828-1840. DOI: 10.1002/aic.16046.

[20] Ramsey BL, Pearson RM, Beck LR, Miyake GM (2017) Photoinduced organocatalyzed atom transfer radical polymerization using continuous flow. Macromolecules 50: 2668-2674. DOI: 10.1021/acs.macromol.6b02791.

[21] Liu X, Lu Y, Luo G (2017) Continuous flow synthesis of polystyrene nanoparticles via emulsion polymerization stabilized by a mixed nonionic and anionic emulsifier. Ind Eng Chem Res 56: 9489-9495. DOI: 10.1021/acs.iecr.7b02352.

[22] Yadav AK, Barandiaran MJ, de la Cal JC (2014) Effect of the polymerization technique and reactor type on the poly(n-butyl acrylate) microstructure. Macromol React Eng 8: 467-475. DOI: 10.1002/mren.201300159.

[23] Chemtob A, Lobry E, Rannée A, Jasinski F, Penconi M, Oliveros E, Braun AM, Criqui A (2016) Flash latex production in a continuous helical photoreactor: releasing the brake pedal on acrylate chain radical polymerization. Macromol React Eng 10: 261-268. DOI: 10.1002/mren.201500060.

[24] Liu Z, Lu Y, Yang B, Luo G (2011) Controllable preparation of poly(butyl acrylate) by suspension polymerization in a coaxial capillary microreactor. Ind Eng Chem Res 50: 11853-11862. DOI: 10.1021/ie201497b.

[25] Song J, Zhang S, Wang K, Wang Y (2019) Synthesis of million molecular weight polyacrylamide with droplet flow microreactors. J Taiwan Inst Chem Eng 98: 78-84. DOI: 10.1016/j.jtice.2018.05.008.

[26] Seike Y, Kamio E, Ono T, Yoshizawa H (2007) Extraction of ethyl ester of polyunsaturated fatty acids by utilizing slug flow prepared by microreactor. J Chem Eng Jpn 40: 1076-1084. DOI: 10.1252/jcej.07WE144.

[27] Kamio E, Seike Y, Yoshizawa H, Matsuyama H, Ono T, Microfluidic extraction of docosahexaenoic acid ethyl ester: comparison between slug flow and emulsion. Ind Eng Chem Res 50: 6915-6924. DOI: 10.1021/ie102207c.

[28] Kashid MN, Gerlach I, Goetz S, Franzke J, Acker JF, Platte F, Agar DW, Turek S (2011) Internal Circulation within the liquid slugs of a liquid–liquid slug-flow capillary microreactor. Ind Eng Chem Res 44: 5003-5010. DOI: 10.1021/ie0490536.

[29] Muranaka Y, Nakagawa H, Masaki R, Maki T, Mae K (2017) Continuous 5-hydroxymethylfurfural production from monosaccharides in a microreactor. Ind Eng Chem Res 56: 10998-11005. DOI: 10.1021/acs.iecr.7b02017.

[30] Watanabe T, Karita K, Tawara K, Soga T, Ono T (2019) Rapid synthesis of poly(methyl methacrylate) particles with high molecular weight by soap-free emulsion polymerization using water-in-oil slug flow. Macromol Chem Phys 1900021. DOI: 10.1002/macp.201900021.

[31] Sander JS, Studart AR (2014) Multiwalled functional colloidosomes made small and in large quantities via bulk emulsification. Soft Matter 10: 60-68. DOI: 10.1039/C3SM51900G.

[32] Xiao J, Wang X, Gonzalez AJP, Huang Q (2016) Kafirin nanoparticles-stabilized Pickering emulsions: microstructure and rheological behavior. Food Hydrocolloids 54: 30-39. DOI: 10.1016/j.foodhyd.2015.09.008.

[33] Asano S, Maki T, Nakayama R, Utsunomiya R, Muranaka Y, Kuboyama T, Mae K (2017) Precise analysis and control of polymerization kinetics using a micro flow reactor. Chem Eng Process 119: 73-80. DOI: 10.1016/j.cep.2017.05.016.

[34] Nagaki A, Miyazaki A, Yoshida J (2010) Synthesis of polystyrenes－poly(alkyl methacrylates) block copolymers via anionic polymerization using an integrated flow microreactor system. Macromolecules 43: 8424-8429. DOI: 10.1021/ma101663x.

[35] Yamamoto T, Fukushima T, Kanda Y, Higashitani K (2005) Molecular-scale observation of the surface of polystyrene particles by AFM. J Colloid Interface Sci 292: 392-396. DOI: 10.1016/j.jcis.2005.05.095.

[36] Telford AM, Paham BTT, Neto C, Hawkett BS (2013) Micron-sized polystyrene particles by surfactant-free emulsion polymerization in air: synthesis and mechanism. J Polym Sci A 51: 3997-4002. DOI: 10.1002/pola.26841.

[37] Yamamoto T (2013) Synthesis of nearly micron-sized particles by soap-free emulsion polymerization of methacrylic monomer using an oil-soluble initiator. Colloid Polym Sci 291: 2741-2744. DOI: 10.1007/s00396-013-3059-x.

[38] Nagao D, Yamada Y, Inukai S, Ishii H, Konno M, Gu S (2015) Quantitative understanding of the self-sharpening of growing polymer particle size distributions in soap-free emulsion polymerization. Polymer 68: 176-182.

[39] Liu B, Fu Z, Han Y, Zhang M, Zhang H (2017) Facile synthesis of large sized and monodispersed polymer particles using particle coagulation mechanism: an overview. Colloid Polym Sci 295: 749-757. DOI: 10.1007/s00396-017-4058-0.

Figure Captions

Fig. 1 Schematic image of the experimental setup for heterogeneous polymerization using a water-in-oil (W/O) slug flow.

Fig. 2 (a) Photographs of the exit tube of the flow reactor when polymerization was performed in the absence of surfactant. (b) Appearance of the sample after collection in an ice bath when the polymerization was performed in the absence of surfactant. The polymerization time (*t*) was over 20 min. Upper and lower phases represent organic and water phases, respectively. (c) Representative SEM image of PMMA particles prepared by a heterogeneous polymerization of MMA using a W/O slug flow at 20 min.

Fig. 3 Effects of addition of Span 85 to the continuous organic phase on the characteristics of heterogeneous polymerization of MMA using a W/O slug flow regarding (a) particle diameter, (b) *CV* of particle diameter, and (c) conversion of MMA. (d) SEM images of PMMA particles prepared with different concentration of Span 85 as a surfactant at different reaction times. The initiator concentration was fixed at 5 mM.

Fig. 4 Effects of initiator concentration in the dispersed water phase on the soap-heterogeneous polymerization of MMA using a W/O slug flow with 5 wt% Span 85 regarding (a) particle diameter, (b) *CV* of particle diameter, and (c) conversion of MMA. (d) SEM images of PMMA particles prepared with different concentrations of initiator at 120 min reaction time.

Table 1 Effects of Span 85 concentration on the interfacial tension of W/O interface and zeta-potential of the resultant PMMA particles.

Span 85 concentration [wt%]	Interfacial tension [mN m^{-1}]	Zeta-potential of PMMA particles [mV]
0	34.0	-49.5
1	24.8	-44.0
5	22.2	-48.0
10	17.6	-41.8

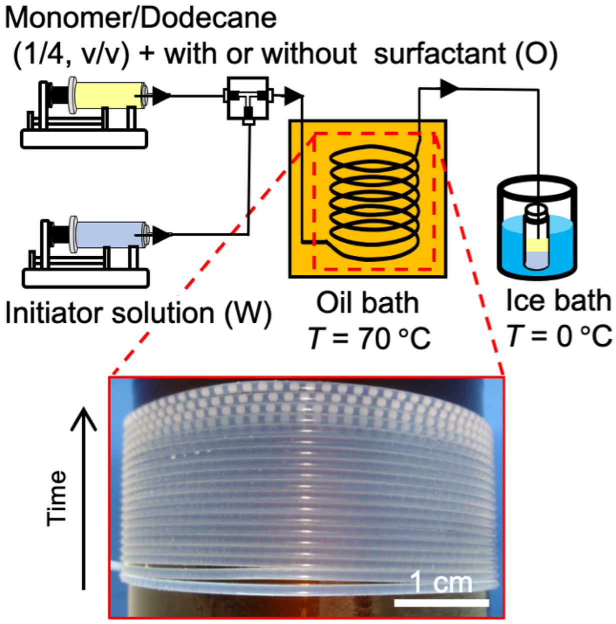

Fig. 1 Schematic image of the experimental setup for heterogeneous polymerization using a water-in-oil (W/O) slug flow.

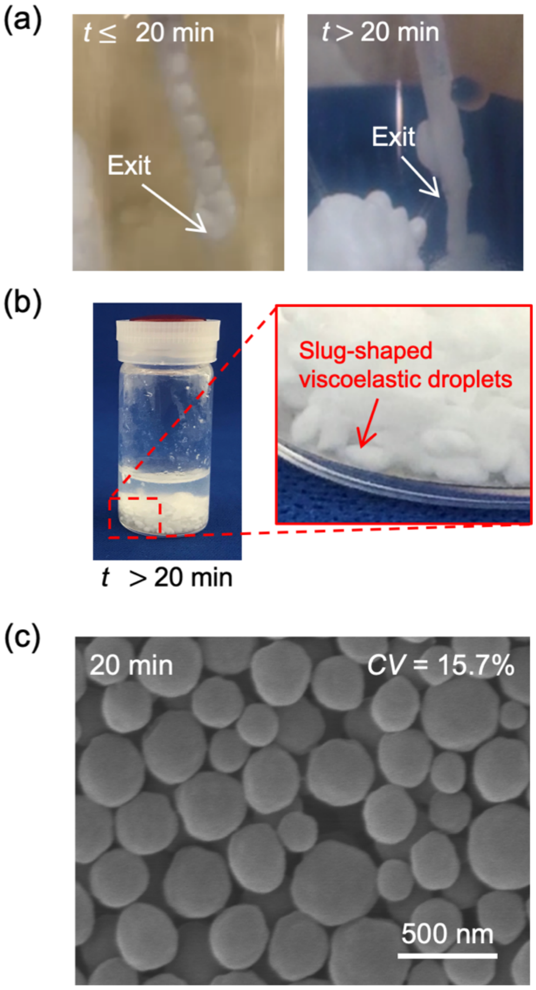

Fig. 2 (a) Photographs of the exit tube of the flow reactor when polymerization was performed in the absence of surfactant. (b) Appearance of the sample after collection in an ice bath when the polymerization was performed in the absence of surfactant. The polymerization time (*t*) was over 20 min. Upper and lower phases represent organic and water phases, respectively. (c) Representative SEM image of PMMA particles prepared by a heterogeneous polymerization of MMA using a W/O slug flow at 20 min.

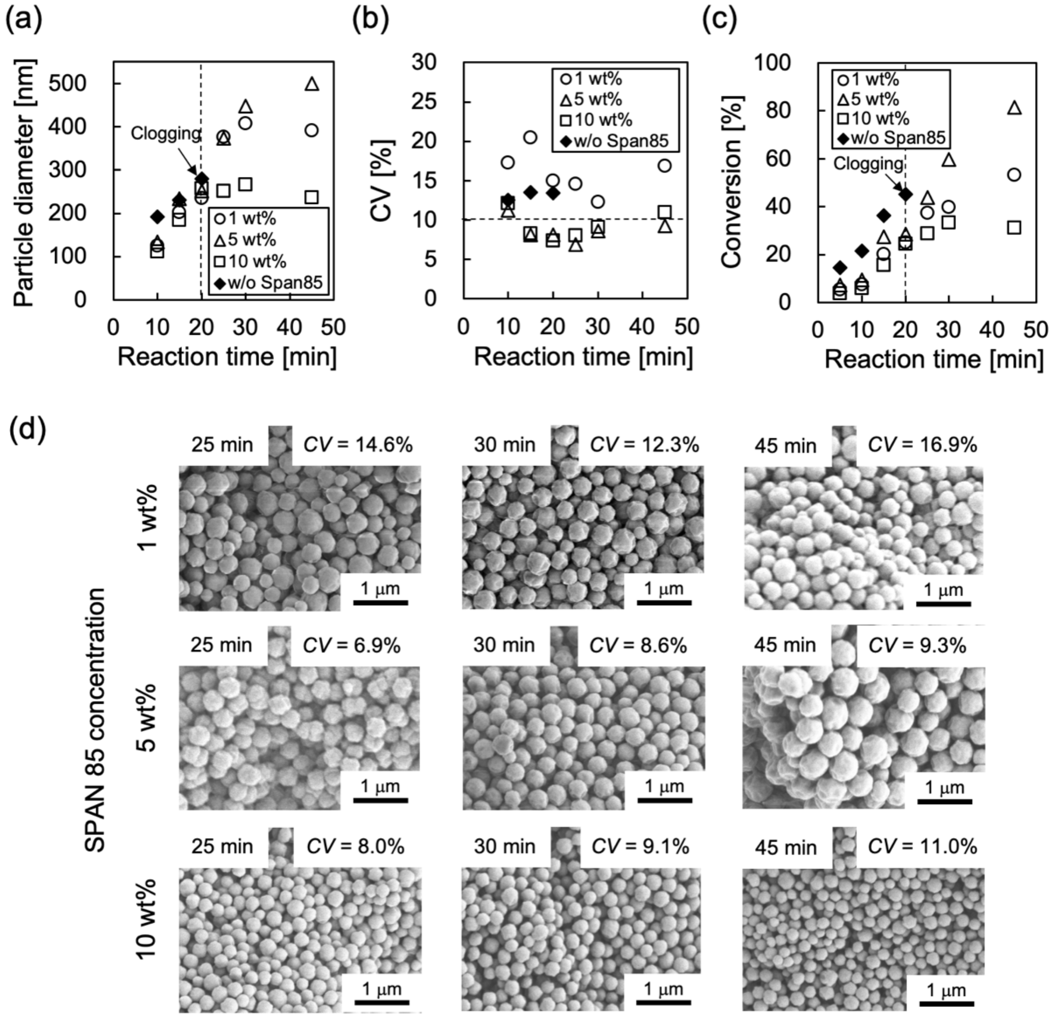

Fig. 3 Effects of addition of Span 85 to the continuous organic phase on the characteristics of heterogeneous polymerization of MMA using a W/O slug flow regarding (a) particle diameter, (b) *CV* of particle diameter, and (c) conversion of MMA. (d) SEM images of PMMA particles prepared with different concentration of Span 85 as a surfactant at different reaction times. The initiator concentration was fixed at 5 mM.

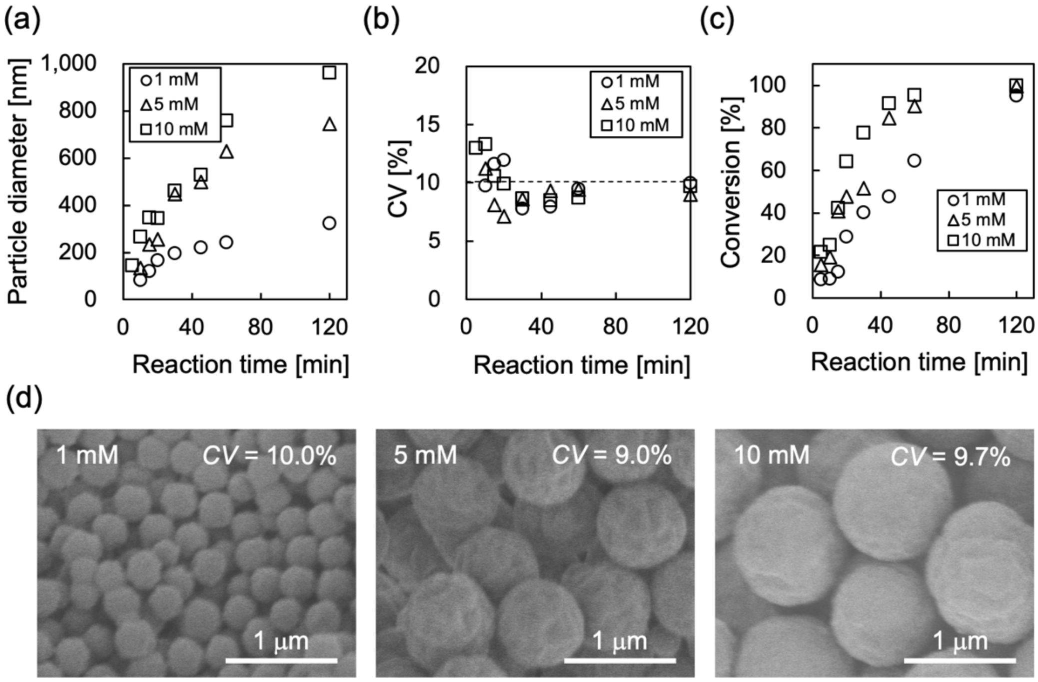

Fig. 4 Effects of initiator concentration in the dispersed water phase on the soap-heterogeneous polymerization of MMA using a W/O slug flow with 5 wt% Span 85 regarding (a) particle diameter, (b) *CV* of particle diameter, and (c) conversion of MMA. (d) SEM images of PMMA particles prepared with different concentrations of initiator at 120 min reaction time.